LOADING ON STRUCTURES FROM FLUIDIZED AVALANCHE FRONTS OVERFLOWING DEFLECTING DAMS AT FLATEYRI, ICELAND, JANUARY 2020

Kristín Martha Hákonardóttir[1,2]*, Ragnar Lárusson[2], Árni Kristjánsson[2], Gunnlaugur Pétursson[2]

[1] *Ministry of the Environment, Energy and Climate, Reykjavík, Iceland*
[2] *Verkís Consulting Engineers, Reykjavik, Iceland*

ABSTRACT: This study back-calculates impact pressures in two dry slab avalanches that were released on a 700 m high mountain above the village of Flateyri in Northwestern Iceland in January 2020. The avalanches were released from distinct starting zones, located east and west of the village. They partially overflowed two 14–20 m high deflecting dams by 150 m and 300 m, respectively. The total mass of the avalanches was estimated $116 \cdot 10^6$ kg and $150 \cdot 10^6$ kg, respectively. Radar measurements, avalanche deposit density, and structural damage suggest that the portion of the avalanches that overran the dams (10% of the total mass) belonged to a fluidized region with intermittent density. Type 1 deposits (dense core) were found upstream of the dams, whereas Type 2 deposits (fluidized flow) were located on the lee side, extending to a maximum run-out position, here termed "T2". Type 3 deposits (suspension) reached the sea. Observations of the Flateyri avalanches provide unique insights into the interaction between powder snow avalanches with a strongly fluidized front and deflecting dams. Furthermore, these observations illustrate the physics of the fluidized front in the run-out zone of the avalanche path, particularly its separation from the denser core by the dams. This paper analyzes damaged structures, back-calculates impact pressures, and discusses periodic pressure pulses and brief compression shocks. The focus is on: (1) a partially snow-filled reinforced concrete house with broken windows and doors, and a damaged roof, located 100 m from the top of the dam; (2) three partially snow filled vehicles that were damaged and moved 13 to 20 m laterally; (3) a steel mast on top of the deflecting dam that was broken in two pieces but not dislocated; (4) the mast's radar antenna that was transported 280 m without damage; and finally (5) a timber shed that shattered, 280 m from the dam and 30 m from T2.

KEYWORDS: Snow avalanches; powder-snow avalanches; snow avalanche deposit; fluidized front; field observations.

1. INTRODUCTION

Fluidized fronts in powder snow avalanches exhibit strong turbulence and flow speeds that exceed those of the dense core. The density distribution is non-uniform both vertically and laterally, and a periodicity characterized by a main frequency of 0.6 Hz has been measured (Sovilla et al., 2015; Lube et al., 2021). The average density of the fluidized part may range from 10^1 to 10^2 kg/m^3 (Sovilla et al., 2018; Issler et al., 2019). The acoustic speed in the fluidized front is possibly an order of magnitude lower than in air, making it comparable to the flow speed. This can result in the occurrence of weak or strong compression shocks during interactions with obstacles (Eglit et al., 2007; Johnson, 2020). Consequently, structures may experience various types of loading from the fluidized flow, including semi-steady dynamic pressure, periodic pressure pulses, and compression shocks. The deposits left by powder-snow avalanches typically exhibit three distinguishable textures (Issler et al., 2019): Type 1: Dense core. The layer is relatively deep, dense, granular, or blocky. Type 2: Fluidized front. Fine grained and shallow, with snow clods, lower density than the dene core, and a longer runout than the T1 deposit. Type 3: Suspension. This layer is less dense, with the longest runout.

In January 2020, two dry slab avalanches were released from the 700 m high mountain above the village of Flateyri in NW-Iceland (see Figure 1). The avalanches originated from separate starting zones, east and west of the village. They partially overflowed two 14–20 m high deflecting dams by 150 m and 300 m, respectively. The mass of the avalanches was estimated to be $(115 \pm 25) \cdot 10^6$ kg and $(150 \pm 25) \cdot 10^6$ kg, respectively, of which $9 \cdot 10^6$ kg and $17 \cdot 10^6$ kg overflowed the dams and at least $17 \cdot 10^6$ kg and $26 \cdot 10^6$ kg flowed into the sea (Hilmarsson et al., 2020; Jóhannesson et al., 2024). Radar measurements of flow speed, and density measurements of the avalanche deposits indicate that the Skollahvilft avalanche was a transitional avalanche of cold snow flowing into a warmer snow cover at lower elevations, with a 400 m long fluidized front flowing at a speed of 45 to 60 m/s towards the dam. This was followed by a denser core traveling at 30 to 45 m/s for approximately 10 s and a slower tail moving at 20 m/s for additional 10 s, exhibiting plug flow behavior (Hilmarsson et al., 2020; Jóhannesson et al., 2024). It is inferred that the portion of the avalanches that overran both dams, comprising about 10% of the total mass, originated from the fluidized front of the avalanche. The flow surpassed the dams, causing

* *Corresponding author address:*
Kristín Martha Hákonardóttir, Ministry of the Environment, Energy and Climate, Reykjavík, Iceland;
tel: ++354 5458600;
email: kristin.hakonardottir@urn.is

damage to one house that was partly filled with snow and where a person was buried, but saved unharmed. Additionally, three vehicles were damaged, a steel mast was broken, a timber shed was destroyed, and shrubs and trees were broken or uprooted. Type 2 debris was found on the lee side of the dams. It was about 0.75 m thick on top of approximately 0.35 m thick layers of older dense snow (see Figure 2 and Figure 3). The deposit was fine-grained and mixed with tree branches, with an average density of 415 kg/m^3. Upstream of the dams, the debris was primarily Type 1 with traces of Type 2 deposit. The debris was blocky and mixed with soil and branches. Next to the dams, it was up to 7 m thick and 10–70 m wide, with an average density of 495 kg/m^3.

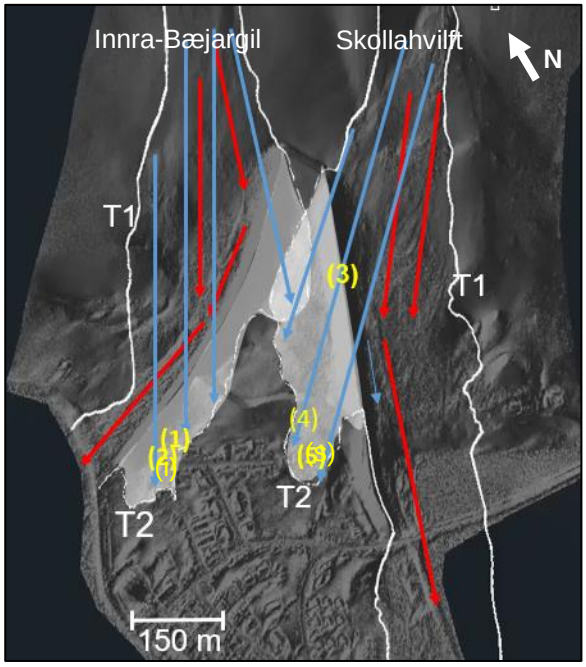

Figure 1: A LiDAR scan by Svarmi of the Flateyri dams and avalanches in January 14, 2020. The outlines of the avalanches are white. The arrows indicate the most likely direction of the avalanche flow (red: dense core; blue: fluidized front), and the numbers correspond to the locations of damaged structures: (1) house at Ólafstún 14, (2) cars, (3) mast, (4) radar, (5) shed. Intact structures: (i) house, (s) gate.

The flow deflected by the Skollahvilft dam reached approximately 10 m vertically on the lower part of the dam, leaving an additional 5 m to the top (see Figure 4). Marks on the dam indicate that the avalanche flowed parallel to it in a thick stream. These marks resemble those observed in the 1999 Flateyri avalanche and were interpreted as the result of an oblique granular jump at the dam face (Jóhannesson, 2001). Granular jumps have been observed in small-scale experiments and reproduced in numerical simulations (Johnson et al., 2020; Pétursson et al., 2019; Jarosch et al., 2022). However, the fluidized flow that surpassed the dams was relatively unaffected by them (blue arrows on Figure 1 and Figure 4).

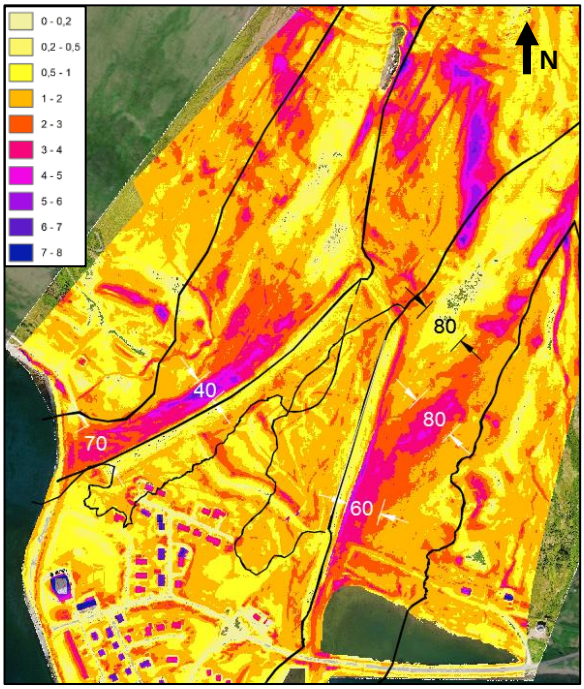

Figure 2: Snow depth on the ground calculated from a LiDAR scan on January 16, 2020. The snow depth includes avalanche debris on top of older snow.

Figure 3: The avalanche debris at the Skollahvilft dam. Left: Type 2 deposit on the lee side of the dam. Right: Type 1 deposit upstream of the dam. The dashed lines indicate the boundary between old snow and deposited snow. Photos: Ó. Hilmarsson.

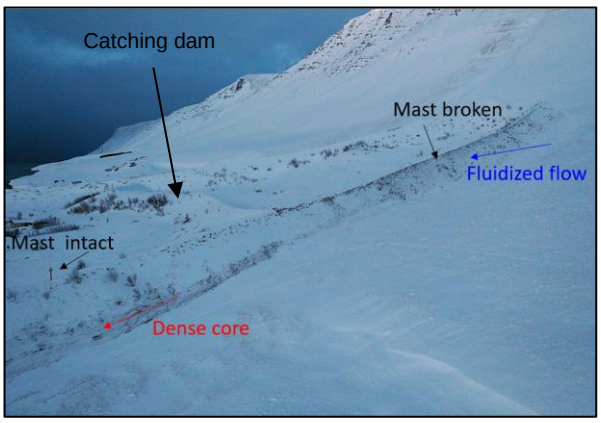

Figure 4: Skollahvilft deflecting dam: Flow marks. The debris thickness is approximately 3–5 by the

dam. The avalanche overran the upper half of the dam. Photo: Verkís, January 2020.

2. THEORY

There are several ways in which the fluidized front may interact with structures and cause damage. Understanding the failure mechanism of structures impacted by such flows is crucial for designing effective mitigation measures. Structures may experience at least the following type of loading: (1) semi-steady dynamic pressure (2) periodic pressure peaks and (3) compression shocks.

2.1 Steady impact pressure

The impact pressure *P* exerted by avalanches on structures is commonly calculated under steady flow conditions using the following equation:

$$P = \frac{F_D}{A} = \frac{1}{2} C_D \rho u^2, \quad (1)$$

where F_D is the drag force on an obstacle, A is the projected impact area of the obstacle, C_D is the drag coefficient, ρ the density, and u is the flow velocity.

The drag coefficient C_D varies with the object's shape and several parameters including the Reynolds number, the Mach number, the Knudsen number, and the Froude number (Issler et al., 2019; Kyburz et al., 2022). The Reynolds number for the fluidized front is estimated Re > 10^5 and C_D = 1–1.5 for a cylindrical mast with a diameter of 0.5 m, in line with discussions by Issler et al. (2019) and C_D = 2 for a flow that stops upon impact.

In avalanche simulations, C_D = 2 is typically used for dense avalanches. Efforts have been made to correlate structural damage caused by avalanches with specific values of impact pressure (Rapin, 2002):

1-4 kPa	Powder snow breaks windows.
>5-10 kPa	Powder snow destroys forest.
3 kPa	Dense avalanche leads to turnaround of a freight car (18 t).
10 kPa	Dense avalanche leads to serious damage of timber structures.
1000 kPa	Dense avalanche leads to movement of reinforced concrete structures.

2.2 Periodic pressure peaks

Repeated pressure peaks, with the most energetic frequency of approximately 0.6 Hz, have been measured in the fluidized front of powder snow avalanches in Switzerland (Sovilla et al., 2018). Similar behavior has been observed in large-scale experiments of pyroclastic flows in New Zealand (Borsch et al., 2021). Borsch et al. (2021) have found that dynamic pressure energy is primarily carried by large-scale coherent turbulent structures and gravity waves, which generate low-frequency, high-pressure pulses downstream. This phenomenon may explain the destructiveness of such flows, as periodic pressure variations can lead to structural failure at lower dynamic pressure values. Such periodic behavior was suggested as a possible cause of the destruction of highly reinforced concrete deflective walls in Taconnaz, France, by a powder snow avalanche in 1999 (Rambaud et al., 2007). Additionally, Bartelt et al. (2018) suggested that periodic dynamic loading by powder snow avalanches (air blasts) might coincide with the main eigenfrequency of tall trees, potentially causing failure at still lower dynamic pressure levels.

2.3 Compression shock

The compressibility of flows is quantified by the Mach number:

$$Ma = \frac{u}{c},$$

where u is flowspeed and c is the acoustic wave speed. In the fluidized front, the acoustic speed may be of the same order as the flow speed, ranging from 10^1 to 10^2 m/s, potentially leading to shockwave formation upon impact with an obstacle (Eglit et al., 2007). Eglit et al. (2007, 2008) derived that compression shocks in low-density avalanches upon impact cause pressure peaks at the initial moments of impact. The magnitude of the pressure peak increases as compressibility increases and the Mach number approaches 1. Issler et al. (2019) estimated the Mach number of the fluidized front of powder snow avalanches to be less than one, or at the most, close to one, indicating subsonic or transonic flow regimes in the fluidized front. In subsonic flow, a weak compression shock may occur upon impact. This results in a brief rise in pressure (Eglit et al., 2008). In supersonic flow, strong compression shocks occur upon impact, and are present during the flow. These shocks are analogous to steady hydraulic jumps in high Froude number incompressible free surface flows. In granular free surface flows, both types of shocks−compression and granular jumps−may coexist and interact (Johnson, 2021). Pressure waves generated by strong compression shocks can be transmitted away from the shock and are experienced as noise, such as sonic booms and sonic crackles (Fwocs Williams et al., 1975; The National Bureau of Standards, 1971).

Here, we focus on structural damage caused by weak impulsive shocks in subsonic or transonic flow. The structural damage depends on both the characteristics of the on-coming flow and the structure. The energy will be absorbed by relatively large and heavy structures without damage. However, these shocks may damage more brittle structures, such as window glass, doors, and unreinforced concrete walls, with higher eigenfrequencies (The National Bureau of Standards, 1971). Impulsive noise and overpressure

have been associated with the following damage (Lees, 1980):

15-85 kPa	Eardrum rupture, 1-90%.
55 kPa	Destruction of buildings.
15-20 kPa	Non-reinforced concrete walls shatter.
3.5-7 kPa	Windows shattered; some frame damage.
0,3 kPa	Loud noise, sonic boom glass failure.

Indications of sudden pressure changes in large avalanches in Iceland include descriptions of people feeling earache in the 1995 Flateyri avalanche as it passed, and more dramatically, eardrum rupture in those who perished in the avalanche (Haraldsdóttir, 2002). In the 2020 avalanches, no such sudden effects due to pressure change were reported. However, residents reported hearing two explosive sounds prior to the arrival of the Skollahvilft avalanche, followed by a deep undertone as it passed. The Innra-Bæjargil avalanche was described as producing a sudden knocking sound on a nearby residential house, as if a car had hit the building.

2.4 Car movement

The force on a car of mass m and projected impact area A, immersed in an avalanche moving with a steady velocity $\boldsymbol{v}$ and having a uniform density distribution ρ, is given by:

$$\boldsymbol{F}(t) = \frac{1}{2}\rho A C_D \left(\boldsymbol{v} - \boldsymbol{u}(t)\right)^2,$$

where $\boldsymbol{u}(t)$ is the car´s velocity at time t, with $\boldsymbol{u}(0)=0$. Applying Newtons second law in the direction of the flow and neglecting basal resistance, the car´s velocity as a function of time is:

$$u(t) = v - \frac{1}{Kt+\frac{1}{v}}, \text{ where } K = \frac{1}{2}\frac{\rho A C_d}{m}. \qquad (2)$$

3. ANALYSIS

3.1 Average density of the fluidized front

We estimate the average density of the fluidized front of the Skollahvilft avalanche to be 40–85 kg/m^3. The estimation is based on the deposited mass of $17 \cdot 10^6$ kg. on the lee side of the dam, with the fluidized flow having a width of 100 m, a length of 400 m, and a thickness of 5–10 m (see Figure 2). Measurements of pyroclastic flows and fluidized avalanches suggest that density decreases upwards through the flow, with periodic increases at higher elevations (Borsch et al., 2021; Sovilla et al., 2018).

3.2 The retarding effect of the dams

The fluidized front passed over the 14–20 m high deflecting dams and the 10 m high catching dam without a notable change in direction (Hilmarsson et al., 2023). Figure 5 depicts a section through the Skollahvilft deflecting dam and the catching dam in the flow direction. Both dams are earth fill dams with a 1:1.25 (horizontal:vertical) upstream slope. The vertical height difference encountered by the front is limited to 8 m, while the top of the dam rises 17 m above the ground. The retaining effect of the dams was limited, based on radar measurements upstream of the Skollahvilft dam and debris thickness upstream of the catching dam.

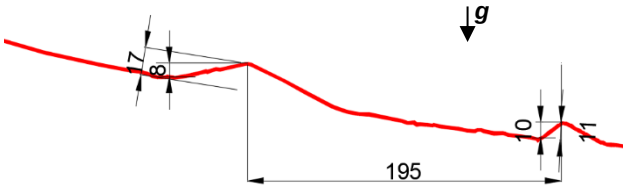

Figure 5: A longitudinal section through the Skollahvilft dams along the flow path of the fluidized front, through the mast (see (3) in Figure 1).

The fluidized front reached a runout of 150 m beyond the Innra-Bæjargil dam and 300 m beyond the Skollahvilft dam. This difference in runout cannot be attributed to a slower avalanche from the Innra-Bæjargil starting zone, as simulations suggest a flow speed of 40 m/s for the dense core of both avalanches. However, the reduced runout may be due to less cold snow in the path of the Innra-Bæjargil avalanche. This reduction could be related to a small avalanche from the gully three days earlier, during a period of heavy snowfall, during which 60% of the new snow from the current snowfall cycle had accumulated. Additionally, the flow's kinetic energy might have decreased significantly due to interactions with the house and cars.

3.3 Displaced cars

Three cars were parked next to the house at Ólafstún 14, approximately 100 m downstream of the Innra-Bæjargil dam (see Figure 1). Two of them, a 1.9 t SUV (marked blue on Figure 6) and a smaller 1.0 t car (red in Figure 6) were transported over a snowpile approximately 3 to 4 m high. They were found upside down about 15 and 20 meters downstream from their original positions, respectively. The blue SUV sustained dents and broken windows, on its downstream side, including two downstream windows and the rear window. A truck (black in Figure 6), which had its rear window facing the avalanche, was moved about 13 m and ended up in a snow pile. It had a broken rear window, was partly filled with light snow, and rotated 90° from its original position.

Through simplified calculations using equation (1), we conclude that the movement of the cars can be contributed to the dynamic force exerted by the fluidized flow (Lárusson et al., 2022). We find that with flow speed of 20 m/s and an average density of 50 kg/m^3, a 1.9 t SUV could be accelerated to a

speed of 14 m/s in 1 s, covering a distance of 10 m This assumes a drag coefficient of 1.5, and a projected impact area of 6.5 m^2.

There is no indication of the cars rolling, which may suggest that the fluidized front had a vertical component or a frontal vortex that contributed to lifting the cars. The cars may also have experienced lift force due to pressure difference over the car.

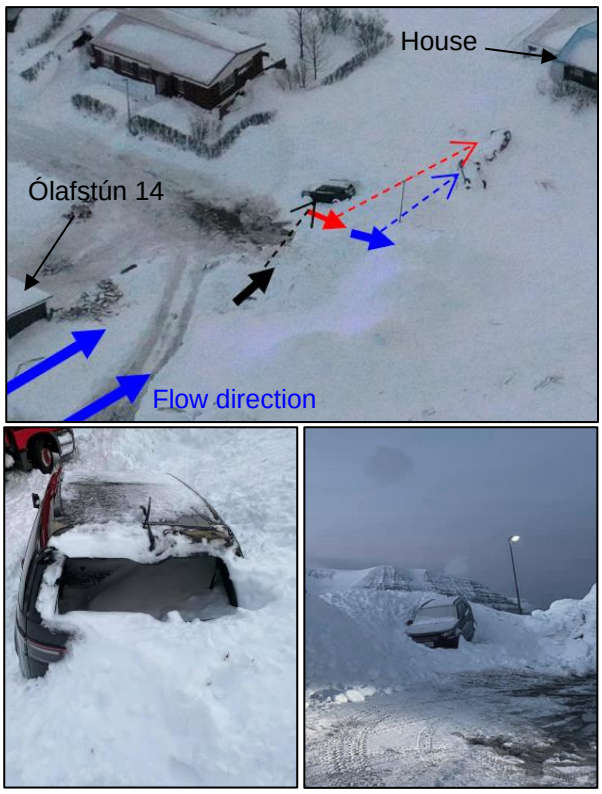

Figure 6: Photos of the three cars after the event. Top: A schematic diagram of the cars' displacement. The two smaller cars (blue and red) were transported 15 m and 20 m, respectively. Bottom: The truck. Photos: K. M. Hákonardóttir and E. Ólafsson.

Transport of cars in powder snow avalanches has been observed in other Icelandic avalanches, including the Þrastarlundur avalanche in East Iceland in 1990. Martinelli and Davidson (1966) reported a similar incident near Berthoud Pass in Colorado in 1964. Dilute air blast from an avalanche transported a 3.2 t truck 19.8 m horizontally and dropped it 15.2 m into a gully causing no significant damage.

3.4 Damaged house

The fluidized front of the avalanche, which overflowed the Innra-Bæjargil dam, interacted with a one-story house at Ólafstún 14, a reinforced, concrete building with a reinforced roof slab and double-glazed windows. It was located approximately 100 m downstream of the Innra-Bæjargil dam. Although there was no structural damage to the house, the upstream side suffered various damages, including to the roof, its edge, broken glass in the windows and a broken door. On the lee side, three windows were broken (two large and one small), along with the front door (see Figure 7 and Figure 8). Estimates of the impact pressure on the house were calculated based on the observed damage and are listed in Table 1. The flow speed at the upstream side of the house was determined to have exceeded 15 m/s in both horizontal and vertical direction. The downstream side does not appear to have experienced significant suction. Therefore, it is inferred that the downstream windows and door broke due to the flow passing through the house, and that the part of the avalanche that flowed over the house had a lower density.

Figure 7: Ólafstún 14. Top: The upstream side of the house. Bottom: Left: The roof edge. Right: Downstream side of the house. Photos: Ó. Hilmarsson and J. Ö. Bjarnason.

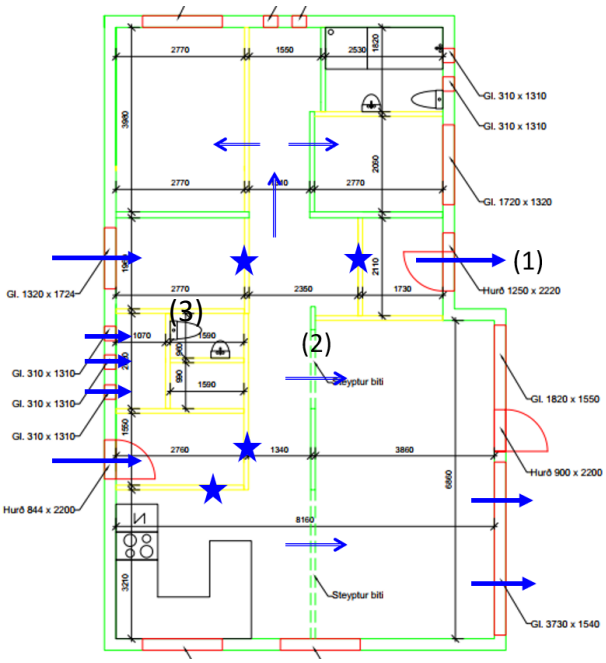

Figure 8: The layout of Ólafstún 14. Blue arrows: The direction of the flow into, through, and out of the house. Blue stars: Broken interior walls. Green lines:

Reinforced concrete walls. Yellow lines: Non-reinforced walls. Red lines: Doors and windows.

Table 1: Bounds on pressure on the upstream and downstream sides of the house.

Upstream side	
Small windows (0.3x1.3 m, 3/4 mm, glass):	> 5/10 kPa
Roof edge (3inch long 75x3.8 mm nails in C18, 150 mm wood boards, 3 nails in each board, 0.8 m between boards):	> 10 kPa
Downstream side	
Small windows (0.3x0.7 m, 3/4 mm, glass)	< 7/12 kPa
Large window (1.8 x 1.5 m, 4 mm glass)	< 2 kPa
Roof edge	< 5 kPa

Photos from inside the house are shown in Figure 9. The following observations were made:

- The kinetic energy of the flow that entered the house through the large window and the back door was sufficient to break the non-reinforced walls, interior doors, and the back door.
- The flow direction through the room (3) and out of the downstream door (1) was relatively direct, and there was more snow accumulation at the door than in the room.
- Snow was found between the books on a bookshelf near the ceiling, even though the room was less than half full of snow.

Figure 9: Photos from inside the house. Left: A shelf near the roof of the house, see (2) in Figure 8. Right: Looking into the house through the downstream door, see (1) in Figure 8. Photos: Ó. Hilmarsson.

We conclude that the flow hit the house at a speed exceeding 15 m/s. The front was 2–3 m thick (main mass of the front) upon hitting the house and may have had a vertical velocity component. The windows and door on the upstream side broke immediately upon impact, possibly due to a brief pressure peak. As the flow passed through the house, it broke non-reinforced walls, the backdoor and three windows on the lee side. Although the flow was turbulent and chaotic, it maintained a consistent direction through the house.

3.5 Broken steel mast and radar

Two 4.1 m high cylindrical steel masts were located on the Skollahvilft dam, equipped with radars to measure avalanche velocities (see Figure 10). The upper mast broke during the avalanche, and the radar antenna was found intact approximately 280 m downstream. Although the mast was cut into two parts, it had not been transported downstream. The steel was slightly deformed and elongated in the assumed direction of the flow. The mast formed a 30° angle with dam, which may be interpreted as the flow direction. The mast was made of 6.3 mm thick St. 52 steel with an outer diameter of 0.22 m. The first and second eigenfrequencies of the mast are 0.4 and 2.6 Hz, respectively.

Figure 10: The radar mast. Top: The mast on the lower (left) and upper (right) half of the dam. Middle: The broken mast. Bottom: A close-up of the broken mast on top of the dam and the radar antenna, 280 m downstream from the mast. Photos: K. M. Hákonardóttir, R. Lárusson and G. H. Halldórsson.

We find that an impact pressure of 60–85 kPa (flow speed of 50 m/s) is sufficient to break the steel mast, given a drag coefficient $C_D = 1.5$ and the vertical pressure distributions on the mast, as shown in Figure 11. However, the mast may have also failed due to fatigue from periodic loading caused by the fluidized front. Additionally, with a frequency of 0.4 Hz, this could lead to 3–4 pressure pulses coinciding with the mast's eigenfrequency (Brosch et al., 2021).

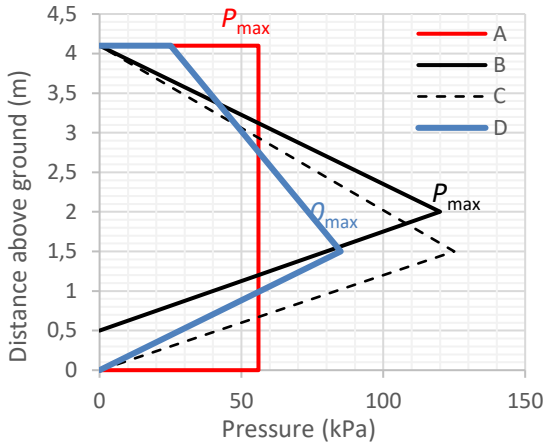

Figure 11: Vertical pressure distribution on the 4.1 m high steel mast for four load cases, A to D, each leading to failure of the steel mast.

The radar antenna was found approximately 280 m downstream from the mast, near the timber shed (see Section 3.6). It was intact, indicating that it did not collide with objects, roll, or ricochet. Similar observations have been reported; for instance, in the 1995 Flateyri avalanche. A box full of books, and a photo album were transported tens of meters and found intact, while the catastrophic avalanche had destroyed everything in its path (Haraldsdóttir, 2002). These observations suggest that the fluidized front may have had a vertical velocity component.

3.6 Broken timber shed

A shed in the Flateyri graveyard was shattered and transported approximately 10 m downstream, coming to rest 30 m from T2. The graveyard gate remained intact (see Figure 12). Despite the damage, the shed's walls stayed relatively intact. Assuming the shed experienced an impact pressure of around 5 kPa, the back-calculated flow speed was 10 m/s.

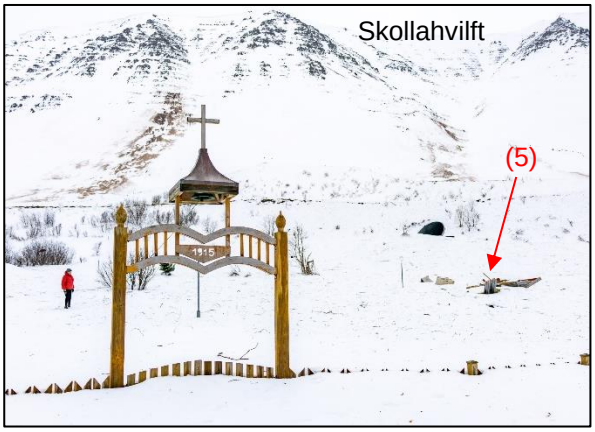

Figure 12: The Flateyri graveyard, looking upstream into the Skollahvilft starting zone. (5) The broken timber shed and the timber gate 35 m downstream from the shed. Photo: Gísli H. Halldórsson, January 19, 2020.

4. CONCLUSIONS

Two avalanches, originating from distinct starting zones, partially overflowed two 14–20 m high deflecting dams by 150 m and 300 m, respectively, causing damage to structures on the lee side of the dams. The avalanches initially began as powder snow avalanches and a strongly fluidized front had developed upon impacting the dams. The following main conclusions regarding the fluidized flow were drawn:

- The fluidized front separated from the denser core at the dams. It approached the Skollahvilft dam at a speed of 45–60 m/s and extended approximately 400 m in length.
- The fluidized front passed over the deflecting dams and the catching dam without significant retarding effects.
- The shorter overflow over the Innra-Bæjargil dam may be due to (a) reduced availability of cold snow in the flow path, caused by a small avalanche three days before the event, and (b) reduction in the flow's kinetic energy during its interaction with the house and cars.

The back-calculated impact pressures on structures due to the fluidized flow are listed in Table 2 and Table 3. Key observations include:

- The observed damage can largely be explained by the dynamic forces exerted on the structures.
- Several observations suggest that the fluidized front had a vertical velocity component.
- The fluidized flow over the Innra-Bæjargil dam was 2–3 m thick (main mass of the front) upon impacting the house at Ólafstún 14.

Observations suggesting impulsive or periodic loading in the 2020 and 1995 Flateyri avalanches include:

- The failure of the radar mast in 2020.
- The immediate failure of upstream doors and windows of the house at Ólafstún 14.
- Reports of eardrum ruptures and earaches in 1995.

Table 2: Back-calculated pressure and flow speed downstream of the Innra-Bæjargil dam (Figure 1).

Innra-Bæjargil dam	*(1) House*	*(2) Cars*	*(i) House*
Dist. from T1 (m)	100-120	100-110	150
Dist. from T2 (m)	20-55	30	0
Imp. pressure (kPa)	>10	15	<2
Flow speed (m/s)	>15	20	<5

Table 3: Back-calculated pressure and flow speed downstream of the Skollahvilft dam (Figure 1).

Skollahvilft dam	*(3) Mast*	*(4) Shed*	*(s) Gate*
Dist. from T1 (m)	20	270	305
Dist. from T2 (m)	300	30	-5
Imp. pressure (kPa)	60-85	5	<2
Flow speed (m/s)	45-60	10	<5

ACKNOWLEDGEMENT

The authors would like to acknowledge the financial support of the Icelandic Avalanche and Landslide Fund and thank the following people for fruitful discussion on fluidized flows: B. Sovilla, SLF; Ó. Hilmarsson and T. Jóhannesson, IMO; P. Gauer and D. Issler, NGI; T. Faug, INRAE UR ETNA; Kouichi Nishimura from the Japanese Society of Snow and Ice; and G. G. Tómasson, Landsvirkjun.

REFERENCES

Bartelt, P., T. Feistl, O. Buser and A. Caviezel. Dynamic magnification factors for tree blow-down by powder snow avalanche air blasts, Nat. Hazards Earth Syst. Sci., 18(3), 759–764, 2018.

Brosch, E., G. Lube, M. Cerminara, T. Esposti-Ongaro, E. C. P. Breard, J. Dufek, B. Sovilla and L. Fullard. Destructiveness of pyroclastic surges controlled by turbulent fluctuations, Nature Communications 12, 7306, 2021.

Eglit, M. E. and V. S. Kulibaba. Numerical modeling of an avalanche impact against an obstacle with account of snow compressibility, Annals of Glaciology 49, 27–32, 2008.

Eglit, M. E., V. S. Kulibaba and M. Naaim. Impact of a snow avalanche against an obstacle. Formation of shock waves, Cold Regions Science and Technology 50, 86–96, 2007.

Ffowcs Williams, J. E., J. Simson and V. J. Virchis. 'Crackle': an annoying component of jet noise, Journal of Fluid Mechanics 71(2), 251–271, 1975.

Hilmarsson, Ó., T. Jóhannesson and H. Grímsdóttir. Snjóflóðin úr Skollahvilft og Innra-Bæjargili 14. Janúar 2020 [The Skollahvilft and Innra-Bæjargil avalanches on January 14th, 2020], The Icelandic Meteorological Office, 2020-010. ISSN 1670-8261, 66 pp., 2020.

Hilmarsson, Ó., K. M. Hákonardóttir, T. Jóhannesson and H. Grímsdóttir. Two severe avalanche cycles in 2020 and 2023 in residential areas in Iceland provide valuable information on avalanche protective structures, in: Proceedings of the Proceedings of the International Snow Science Workshop, Bend, Oregon, 8-13 October, 819–821, 2023.

Haraldsdóttir, S. H.: Snjóflóðasaga Flateyrar og Önundarfjarðar [The Flateyri and Önundarfjörður avalanche chronology], The Icelandic Meteorological Office, ÚR24, Reykjavík, 2002.

Issler, D., P. Gauer, M. Schaer and S. Keller. Inferences on Mixed Snow Avalanches from Field Observations, Geosciences, 10, 2, 31 pp., doi:10.3390, 2020.

Jarosch, A. H., T. Jóhannesson, K. M. Hákonardóttir, and H. Ö. Pétursson: Full three-dimensional simulations of snow-avalanche flow with two-phase, incompressible, granular μ(I) rheology using OpenFOAM / interFoam, EGU General Assembly 2022, Vienna, Austria, 23-27 May 2022, EGU22-7984, https://doi.org/10.5194/egusphere-egu22-7984, 2022.

Johnson, C. G.: Shocking granular flows, J. Fluid Mech., 890:F1, doi:10.1017/jfm.2020.61. 2020.

Jóhannesson, T.: Run-up of two avalanches on the deflecting dams at Flateyri, northwestern Iceland, Annals of Glaciology 32, 350–354, 2001.

Jóhannesson, T. J., H. Grímsdóttir, K. M. Hákonardóttir, S. Brynjólfsson, Ó. Hilmarsson and A. H. Jarosch: Lessons from several avalanches impacting avalanche protective structures in Iceland in January 2020 and March 2023, in: International Snow Science Workshop 2024 Proceedings, Tromso, Norway, Montana State University, 2024.

Kyburz, M.L., B. Sovilla, J. Gaume and C. Ancey. Physics-based estimates of drag coefficients for the impact pressure calculation of dense snow avalanches, Engineering Structures 254(113946), https://doi.org/10.1016/j.enstruct.2021.113478, 2022.

Lárusson, R., K. M. Hákonardóttir and H. E. Hafsteinsson. Vehicle damage and transport and possible shock wave formation in the Flateyri avalanche in January 2020, EGU General Assembly 2022, Vienna, Austria, 23-27 May 2022, EGU22-8220, https://doi.org/10.5194/egusphere-egu22-8220. 2022.

Lees, F. P. Loss Prevention in the Process Industries, 1, Butterworths, London and Boston, 674 pp., 1980.

Martinelli Jr., M. and K. D. Davidson. An example of damage from a powder avalanche, Hydrologival Science Journal 11(3), 26–34, 1966.

Pétursson, H. Ö., K M. Hákonardóttir. and Á. Thoroddsen. Use of OpenFOAM and RAMMS::Avalanche to simulate the interaction of avalanches and slushflows with dams. In: Proceedings of the International Symposium on Mitigative Measures against Snow Avalanches and Other Rapid Gravity Mass Flows., Siglufjörður, Iceland, 3-5 April, 183–195, 2019.

Rambaud, P.B., A. Limam, P. Roenelle, F. Rapin, J.-M. Tacnes and J. Mazars. Avalanche action on rigid structures: Back-analysis of Taconnaz deflective walls' collapse in February 1999, Cold Regions Science and Technology 47, 16–31, 2007.

Rapin, F.: A new scale for avalanche intensity, in: Proceedings of the 2002 International Snow Science Workshop, Penticton, British Columbia, 29 September-4 October 2002, 90–96, 2002.

Sovilla, B., J. McElwaine and M. Y. Louge. The structure of powder snow avalanches, C. R. Physique 16, 97–104, 2015.

Sovilla, B., J. McElwaine and A. Köhler. The Intermittency Regions of Powder Snow Avalanches, Journal of Geophysical Research: Earth surface 123, 2525–2545, doi:10.1029, 2018.

The National Bureau of Standards. The effects of sonic boom and similar impulsive noise on structures, The U.S. Environmental Protection Agency Office of Noise Abatement and Control Washington, D.C. 20460, December 1971.